Conf-740637--4

HEAVY-ION-INDUCED FISSION

F. Plasil
Oak Ridge National Laboratory*
Oak Ridge, Tennessee 37830

I. Introduction

In nuclear physics, during the last few years, two fields of research have grown in popularity to an almost spectacular extent. First, we have witnessed the growth of interest in heavy-ion reactions, spurred on in part by the possibility of the production of superheavy elements, and by the advent of a new generation of heavy-ion accelerators. Second, there has been a simultaneous revival in the field of fission, stimulated by theoretical and experimental investigations of the double-humped fission barrier [1]. It is, therefore, natural that heavy-ion-induced fission, which is an area of research that lies at the crossroads of these two popular fields, should receive increasing attention. We also concern ourselves with heavy-ion fission because fission plays an important role in heavy-ion reactions, not only in the traditional heavy-mass region, but in fact, in all regions of the nuclear mass table. This is due to a feature that dominates this field: the dramatic lowering of the fission barrier with increasing angular momentum. The consequences of this increased fissility are far-reaching, and go well beyond the traditional limits of fission investigations. To mention just one example, it is likely that under some conditions, evaporation-residue cross sections in the medium-mass region may be limited by fission competition in the compound nucleus de-excitation process [2,3].

Heavy-ion-induced fission was first studied in a systematic way in the late fifties and early sixties. While it is not possible for me to cite all the work that was carried out at that time, I would like to pay special tribute to T. Sikkeland and his co-workers, who at that time laid the experimental foundations of the field by investigating such varied aspects as kinetic energies [4], excitation functions [5-7], angular correlations [8,9], and angular distributions [10]. At about the same time, several theoretical investigations of angular momentum effects on fission barriers were in progress [11-13], including computer calculations in the rotating liquid drop model of Cohen, Plasil and Swiatecki [14,15], which I shall discuss later.

In the limited time available, it is not possible for me to review all aspects of heavy-ion-induced fission, and thus it is necessary for me to highlight certain topics. After these introductory remarks, in section II, I shall review the theoretical basis for the lowering of fission barriers with increasing angular momentum. Further theoretical studies which make use of the barrier calculations of section II to describe fission competition in the de-excitation of compound nuclei will be described in section III and some comparison with experimental results will be made. In section IV we will discuss fission excitation functions for relatively light compound systems ranging from ^{181}Re down to ^{127}La. We will also examine the extent to which the excitation functions can be described theoretically. The succeeding section (section V) will deal with fragment kinetic energies and mass distributions in heavy-ion-induced fission. In the final section (section VI) experimental results relating to non-compound nucleus and "quasi" fission will be examined.

Before I continue, I would like to describe the sequence of events for close" or "hard" heavy ion collisions shown in fig. 1, and to define appropriate erminology. Let us consider a collision between a heavy ion and a target nucleus ith an impact parameter small enough that more than just nuclear surface effects

Operated by Union Carbide Corporation for the U. S. Atomic Energy Commission.

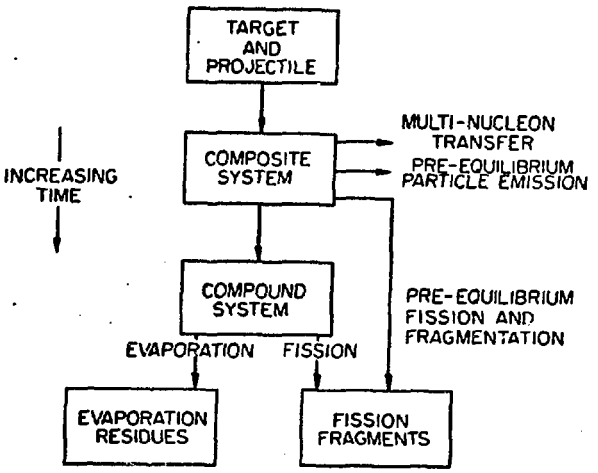

Figure 1. Sequence of events for "close" or "hard" collisions.

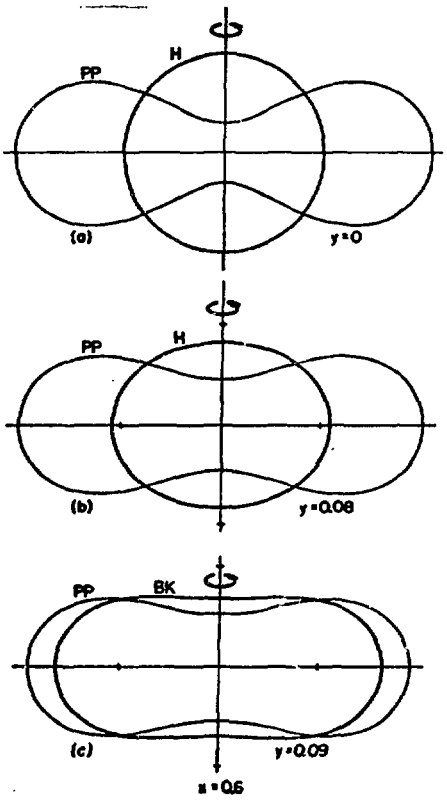

Figure 2. Ground states (heavier lines labeled H or BK) and saddle shapes (lighter lines labeled PP) for X = 0.6 and various values of y. The shapes labeled H have axial symmetry about the vertical axis. The shapes labeled PP and BK have approximate symmetry about the horizontal axis. This figure is taken from ref. 15.

come into play. (By this condition I mean to exclude such reactions as elastic and inelastic scattering, stripping and few-nucleon transfer reactions). The first thing that happens is that the target and projectile form what may be called a "composite nucleus" [15]. In this system the target and projectile have more or less amalgamated, but equilibrium in all degrees of freedom has not been

achieved. Several events can then follow. The system can decay by pre-equilibrium particle emission, or a multi-nucleon transfer reaction can take place, or "fast" or "direct" pre-equilibrium fission can occur. Should the composite nucleus, however, survive long enough to attain equilibrium in all degrees of freedom, the compound nucleus is produced [16]. This can then in turn decay by nucleon evaporation, resulting in evaporation residue products, or by fission. The point to note is that fission fragments can result from the fission of both the compound and the composite nucleus. To complicate matters further, it is not clear that it is possible to distinguish the two types of fission from each other. Whether or not differences are detectable experimentally will depend on the length of time the composite nucleus exists before it fissions. Pre-equilibrium fission involves full momentum transfer from the projectile to the composite nucleus and thus angular correlation measurements [8,9] will not distinguish it from compound nucleus fission. Furthermore, direct fission may involve similar charge and mass distributions as compound fission if the composite nucleus has had time to equilibrate in the relevant degrees of freedom that determine these distributions. Perhaps the most promising way to differentiate between the two types of fission is by means of angular distribution measurements. Times of rotation are estimated to be about an order of magnitude longer than times associated with mass vibrations [17] and this may be long enough for fast fission to occur before one nuclear rotation has taken place. The possibility that fission fragments may originate from either compound-nucleus or composite-nucleus fission should be in the back of our mind whenever we consider any aspects of heavy-ion-induced fission.

II. Theoretical Fission Barriers of Rotating Nuclei

In this section I would like to describe the theoretical basis for the decrease in fission barriers with increasing angular momentum. An early study of this effect, valid in a limited region of nuclei, was carried out by Pik-Pichak [11]. Somewhat later a more extensive study was made by Cohen Plasil and Swiatecki [14,15], and I would like to present some of their results here. The calculations were performed in the rotating liquid drop model, with restrictions to shapes of axial symmetry. The effective potential energy of the drops, from which configurations of equilibrium were obtained by differentiation, consisted of a linear combination of the surface energy, the Coulomb energy and the rotational energy. The rotational energy was given by the square of the angular momentum divided by twice the rigid body moment of inertia. Thus the configurations were confined to gyrostatic equilibrium with all fluid elements in uniform rotation about a common axis. Parametrization of the system was made by means of Legendre polynomials, and equilibrium conditions were obtained in terms of two dimensionless parameters x and y. The fissility parameter x is given by the ratio of the Coulomb energy of a spherical drop to twice its surface energy ($x \approx Z^2/50A$), and y is the ratio of the rotational energy of a sphere to its surface energy ($y \approx 2\ell^2/A^{7/3}$, where ℓ is the angular momentum).

Examples of ground state (stable) and saddle-point (unstable) shapes of equilibrium are shown in fig. 2 for $x = 0.6$. This value of fissility parameter corresponds to nuclei in the region of ytterbium. In the top part of the figure the stable spherical nucleus and the non-rotating elongated saddle-point nucleus are shown for zero angular momentum ($y = 0$). As the rotational energy increases, the ground-state nucleus flattens and maintains axial symmetry about the axis of rotation, while the saddle-point nucleus contracts slowly and thickens its neck. This situation is shown in the central portion of the figure for $y = 0.08$. If rotation is increased still further (provided that $x \lesssim 0.8$), the ground state pseudospheroid loses stability and undergoes a conversion to a triaxial shape resembling a flattened cylinder with rounded edges. Such a shape is shown in the lowest section of fig. 2 for $y = 0.09$. As the angular momentum continues to increase, a point is reached at which the stable and unstable families of equilibrium shapes merge, and the fission barrier vanishes.

In fig. 3 fission barriers from ref. 15 are shown as a function of x and y, in units of the surface energy of a spherical nucleus. It can be seen that for any given nucleus (defined by its value of fissility parameter x), if the angular momentum is sufficiently large, the fission barrier is reduced to zero. This point is illustrated more explicitly in fig. 4 which gives the $B_f = 0$ limit as a function of the familiar variables of angular momentum (units of $\hbar$) and mass number A for nuclei in the valley of β-stability. It can be seen that if the angular momentum is $\gtrsim$ 100$\hbar$, all nuclei have a fission barrier equal to zero. For purposes of estimating competition between fission and particle emission (see section III), it is sufficient that the fission barrier be small compared to the binding energy of individual nucleons in order for fission to dominate. The shaded region divides the diagram roughly into two parts: above the shaded line compound nuclei are expected to de-excite primarily by fission and below it primarily by particle emission.

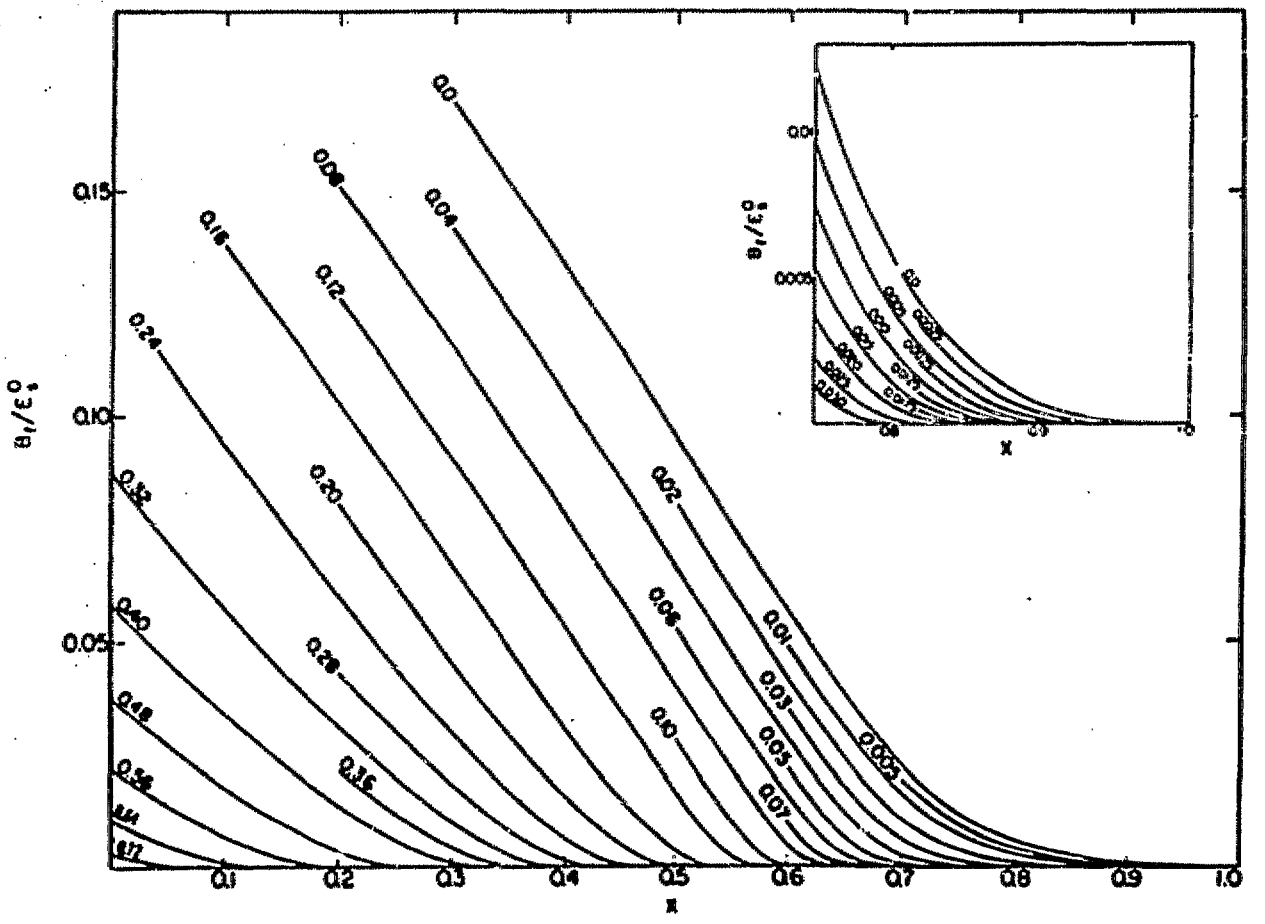

Figure 3. Calculated fission barriers in units of the surface energy of a spherical nucleus as a function of the fissility parameter x for various values of y. Note that for all values of x, the barrier vanishes, provided that y is sufficiently large. This figure is similar to figures of ref. 15.

Figure 5 shows the energies of rotation of the saddle-point and the ground state nuclei for the specific case of the ^{149}Tb compound nucleus. (This nucleus can be obtained in the reaction ^{109}Ag + ^{40}Ar → [^{149}Tb]*, and data for this system will be presented later). It can be seen that as the angular momentum is increased, both the ground-state rotational energy E_R^{min} and the saddle-point rotational energy E_R^{saddle} increase, but that the rate of increase is smaller in the E_R^{saddle} case than in the E_R^{min} case. The difference between the two curves is the fission barrier, B_f, and is also shown. The point of this figure is to examine the extent to which the lowering of B_f with angular momentum is dependent on the

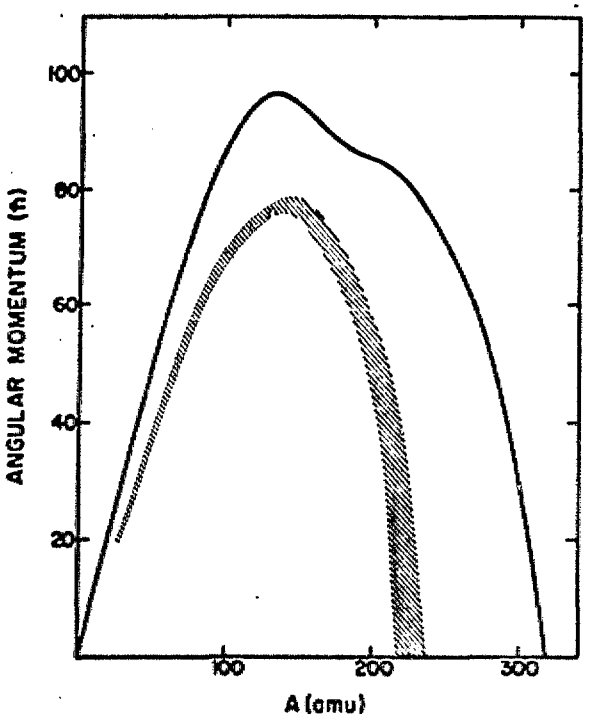

Figure 4. The solid line gives the value of angular momentum at which the fission barrier of beta-stable nuclei of mass number A is predicted to vanish. The hatched area indicates the region of competition between fission and particle emission (see text).

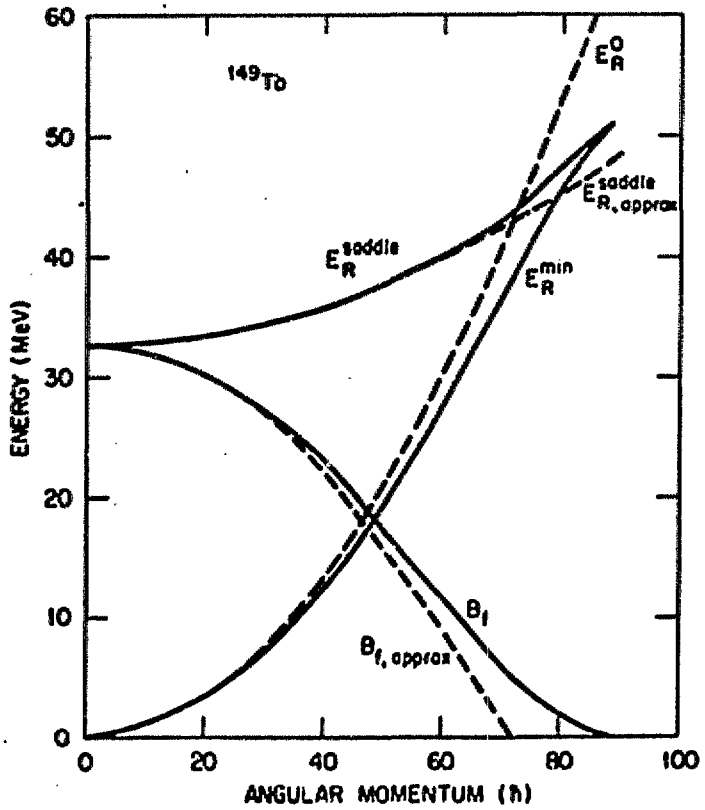

Figure 5. Rotational energies (from the liquid drop model [15]) of the rotating ground state (E_R^{min}) and of the rotating saddle shape (E_R^{saddle}) as functions of angular momentum for ^{149}Tb. The difference between E_R^{saddle} and E_R^{min} is the fission barrier B_f, and is also shown. For further details and for an explanation of the dashed curves, see the text.

specific assumptions of the liquid drop model. For this purpose, let us consider nuclei that are constrained to their non-rotating shape, i.e., nuclei that are not allowed to deform with increasing angular momentum. The rotational energies of such nuclei are given by the dashed lines E_R^o (rotational energy of a sphere) and $E_{R,approx}^{saddle}$. The approximate dependence of the fission barrier on angular momentum is given by the difference between these two curves and is indicated by $B_{f,approx}$. One could argue, however, that the assumed shape of the non-rotating saddle-point nucleus is itself given by the liquid drop model. While this is true in the above illustration, all that is required is that the moment of inertia of the saddle-point shape be substantially larger than the moment of inertia of the ground state. There is independent experimental evidence that this is in fact the case [18].

III. De-excitation of Compound Nuclei with Large Angular Momenta

The calculations that I will describe in this section make use of the angular momentum-dependent fission barriers of the previous section to predict the fate of rotating compound nuclei. Let me stress that these calculations do not shed any light on the crucial question as to whether or not a compound nucleus can be produced for any given set of collision conditions. Rather, the calculations attempt to answer the question: If compound nuclei were produced with a given angular momentum distribution, what fraction would de-excite by fission, and what fraction by particle emission? These calculations can, however, be used to predict evaporation residue cross sections σ_{ER}, provided that entrance conditions are not the limiting factor.

The calculations were performed in collaboration with M. Blann, and have been fully described elsewhere [2,3,19]. As the first step, a distribution of partial cross sections for a given heavy ion reaction is calculated by means of the parabolic-potential approximation of Thomas [20]. The de-excitation calculation is then carried out for each partial wave by considering multiple neutron, proton and α emission in competition with fission at each step of the evaporation cascade. Evaporation probabilities are obtained by means of the Weisskopf-Ewing [21] formalism with appropriate weighting over spectra of residual excitations, and the Bohr-Wheeler [22] expression is used for fission widths. A more detailed description, including several comparisons with experimental results, is given in ref. 3, and the computer program is available to those interested [19].

In fig. 6 results of the calculation at two bombarding energies are shown for the case of $^{109}Ag + {}^{40}Ar \rightarrow [{}^{149}Tb^*]$. The variation of B_f with angular momentum is also indicated. The distribution of partial cross sections is given by the heavy solid lines, and the fission cross section as a function of angular momentum is given by the light lines. It can be seen that fission is expected to play a significant role only above 50 $\hbar$, when the fission barrier has dropped to about half of the value it has at zero angular momentum. Furthermore, the fission cross section in the 180-MeV case is expected to be relatively small when compared with the 288-MeV case, since the partial wave distribution ends at about 70 $\hbar$ in the 180-MeV case and at 135 $\hbar$ in the 288-MeV case.

I will present only two comparisons with experiment here: one in which the calculation adequately describes experimental results, and one in which it does not. Figure 7 gives results of an experiment we have performed at the Berkeley Superhilac in collaboration with the Gesellschaft für Schwerionenforschung, the University of Rochester and Los Alamos Scientific Laboratory [23]. The open circles give measured σ_{ER} values for the de-excitation of ^{149}Tb compound nuclei produced in bombardments of ^{109}Ag with ^{40}Ar. The closed circles give values of $(\sigma_{ER} + \sigma_f)$, where σ_f is the fission cross section. The heavy solid line gives the calculated total reaction cross section, and the light solid line gives the results of our calculation for the evaporation residue cross section. Thus the open circles are expected to lie on the σ_{ER} curve, which, within experimental errors, is in fact the case. Our calculation, however, predicts a slight

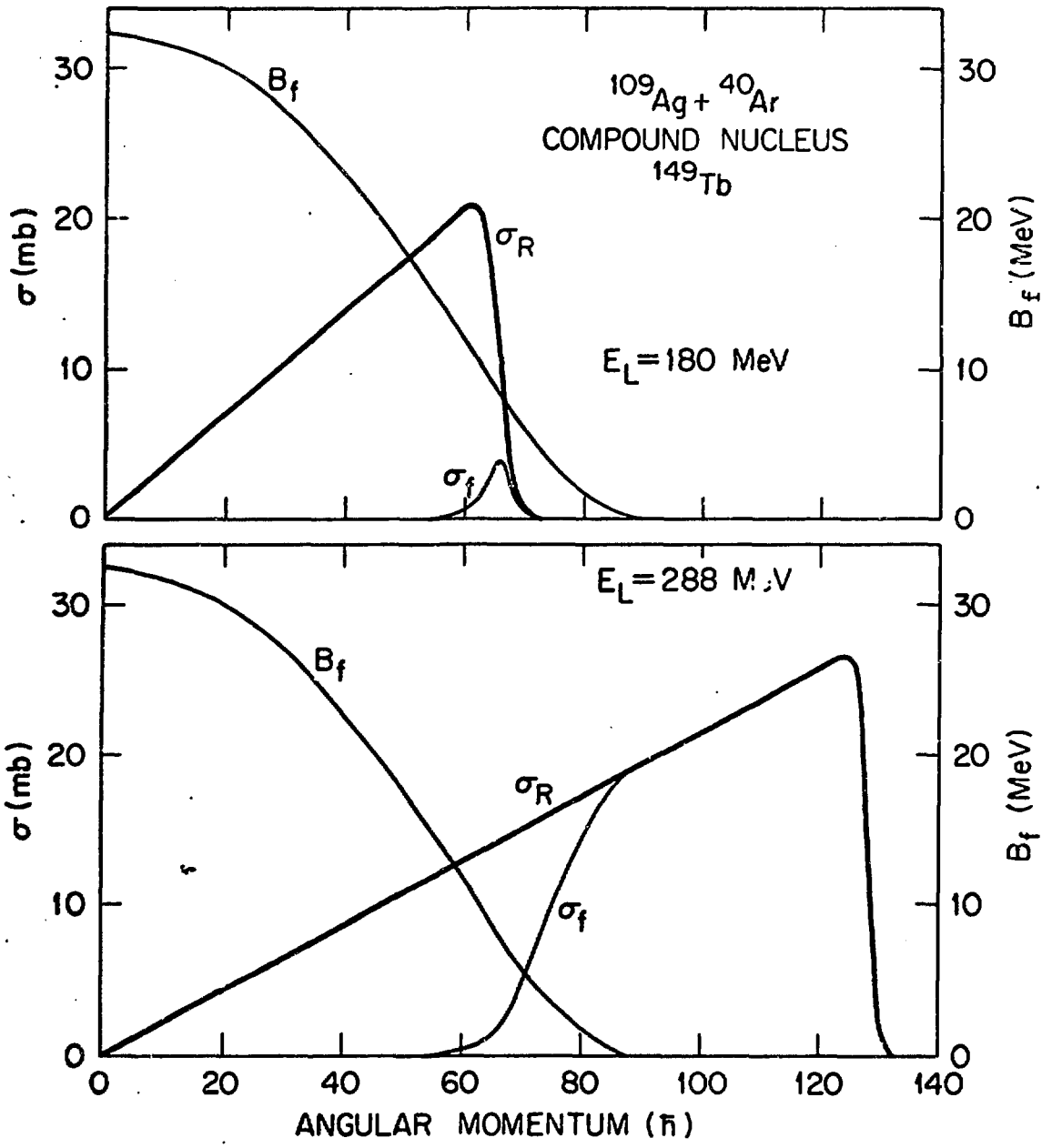

Figure 6. Role of fission in the $^{109}Ag + ^{40}Ar$ reaction at bombarding energies of 180 and 288 MeV according to Blann and Plasil [2,3]. The heavy solid curve gives the distribution of partial waves for the total reaction cross section. The σ_f curve gives the calculated fission cross section. It can be seen that fission is much more important in the 288 MeV case than in the 180 MeV case. The calculated fission barrier is also shown for reference.

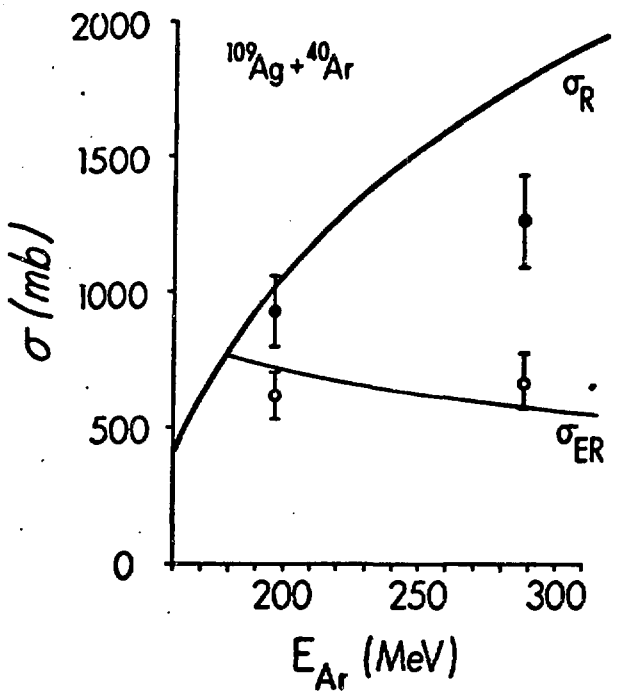

Figure 7. Comparison of experimental results of ref. 23, with calculations [3]. σ_R is the calculated total reaction cross section, and σ_{ER} is the calculated cross section for evaporation residue products. The open circles are measured σ_{ER} values. The closed circles represent the sum of measured evaporation residue and fission cross sections.

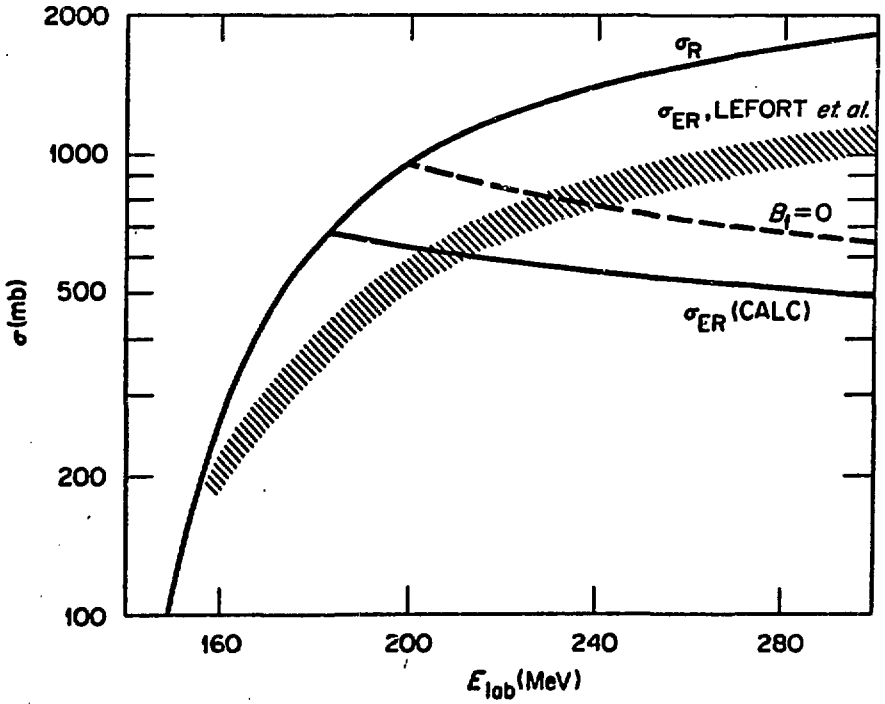

Figure 8. Similar to fig. 7. The hatched area represents the region of experimental results [25,26]. The dashed line provides an indication of where the fission barrier is expected to vanish.

decrease of σ_{ER} with increasing bombarding energy, while the two experimental points indicate a slight trend in the opposite direction. When the measured fission cross section is added to σ_{ER}, it is found that at the lower bombarding energy (E_{lab} = 198 MeV) the estimated total reaction cross section is accounted for. At the higher bombarding energy, however, it can be seen that about 500 mb remain to be accounted for. There are preliminary indications that transfer reactions account for a large fraction of this remaining cross section [24].

Disturbing results for a system similar to the one discussed above, $^{121}Sb + ^{40}Ar$, are given in fig. 8. Calculated σ_R and σ_{ER} curves are again shown, and experimental results of Lefort et al. [25,26] are indicated by means of the shaded region. There is disagreement between theory and experiment in both the trend with bombarding energy and in the absolute magnitude of the cross sections at most bombarding energies. Also shown is a curve corresponding to $B_f = 0$. Above $E_{lab} \approx 240$ MeV, the measured evaporation residue cross sections fall in a region where the fission barrier is predicted to be zero. This represents a serious discrepancy. There is some possibility, however, that the experimental data may be in error. They were obtained by means of post-irradiation γ-ray measurements and are subject to uncertainties in branching ratios and in detection efficiency. In fact the data seem in conflict with those of Fig. 7. At 288 MeV, we obtained a value of σ_{ER} of 700 mb for $^{109}Ag + ^{40}Ar$ while Lefort's σ_{ER} at the same energy, but for a somewhat different system ($^{121}Sb + ^{40}Ar$), is greater than 1000 mb. More experimental data are needed to clear up this situation.

IV. Fission Excitation Functions

A large number of fission excitation functions for heavy-ion-induced fission has been measured during the last fifteen years [5-7,27-30]. For target nuclei lighter than gold, attempts have been made by Sikkeland et al. [5,6] to extract fission barriers from the steep parts of the excitation functions, where fission competes with particle emission. For targets heavier than gold, fission accounts for most of the reaction cross section and fission barriers cannot be extracted. In this section we shall re-examine Sikkeland's data for the ^{181}Re compound nucleus [5], and we shall also discuss more recent results [31-33] for compound nuclei ^{153}Tb and ^{127}La.

There are two main reasons why we shall restrict our attention to compound nuclei with mass numbers between 127 and 181. First, theoretical treatments by which it may be possible to extract fission barriers from experimental data are based on the assumption that all observed fission fragments originate from the fission of de-exciting compound nuclei (see section I). As is indicated by angular correlation experiments [8], in heavy-ion-induced fission this is more likely to be the case for systems with mass numbers below 200, where the fission cross section is a relatively small fraction of the total reaction cross section. Second, for systems having mass numbers less than about 100 (below the so-called Businaro-Galone point [34]), it is predicted that the fragment mass distribution is no longer peaked at symmetric mass divisions. It is possible that in this region of very light fissioning systems the most probable mass divisions are, in fact, so asymmetric as to make it difficult to distinguish fission from deep inelastic transfer processes.

Figure 9 is taken from Sikkeland's original paper [5] and gives the fission probability for the three reactions $^{159}Tb + ^{22}Ne$, $^{165}Ho + ^{16}O$ and $^{169}Tm + ^{12}C$. The method of analysis used by Sikkeland to extract fission barriers makes use of several approximations that may have a serious effect on the extracted B_f values. By using the nuclear de-excitation program ALICE [3,19], it is now possible to carry out the analysis with fewer approximations. We have, therefore, re-analyzed the excitation functions for the three reactions mentioned above in an effort to examine the degree of confidence that one can have in published fission barriers obtained from heavy-ion data. The following changes relative to Sikkeland's method were made in the analysis: (i) Sikkeland accounted for the

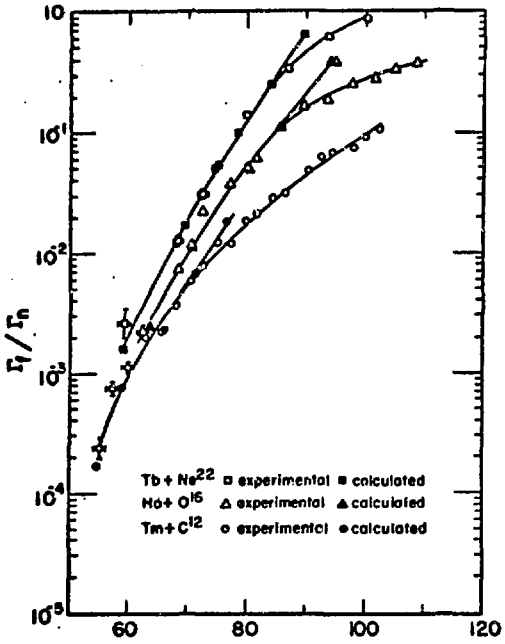

Figure 9. Calculated and experimental ratios of the fission width Γ_f to the neutron emission width Γ_n as a function of excitation energy in MeV for the ^{181}Re compound nucleus formed in three different ways as indicated in the figure. This figure is taken from ref. 5.

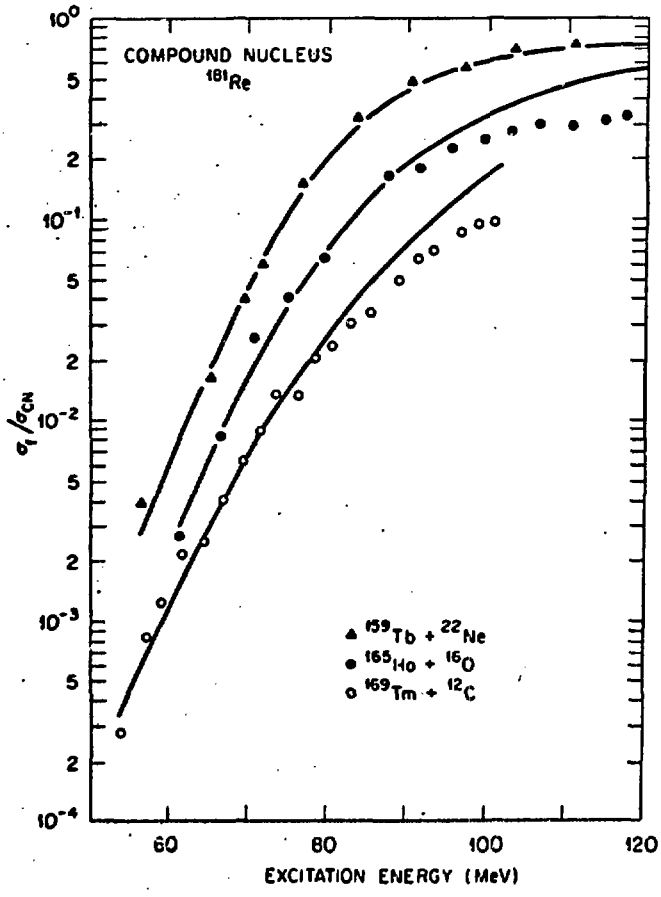

Figure 10. Experimental and calculated values of the ratio of the fission cross section to the compound nucleus cross section for three reactions all producing the compound nucleus ^{181}Re. Parameters associated with the fits are given in table I under the heading: "This work, $\sigma_{CN} = f\sigma_R$." Calculations were performed by means of the computer code of ref. 19.

lowering of the fission barrier with angular momentum by subtracting the rotational energy of the non-rotating saddle-point configuration from the total excitation energy. We have used the angular momentum dependence of the fission barrier as given by the liquid drop model calculations. (ii) The angular momentum correction was applied by Sikkeland only for the average value of angular momentum, while our calculation was carried out separately for each partial wave. (iii) In ref. 5 only first-chance competition with neutron emission was considered, while we have included the possibility of multiple-chance fission and charged particle evaporation.

In addition to the approximations listed above, it was necessary for Sikkeland to estimate values of σ_{CN}/σ_R, where σ_{CN} is the cross section for compound nucleus formation and σ_R is the total reaction cross section. Based on rather sparse experimental results, Sikkeland assumed that σ_{CN}/σ_R is 0.72 for bombardments involving ^{12}C and ^{16}O ions and 0.6 for ^{22}Ne ions. He also assumed that σ_{CN}/σ_R was independent of target and bombarding energy. These assumptions are very likely to be unsatisfactory, but in the absence of additional data, we have decided to perform two sets of calculations, one with Sikkeland's assumed σ_{CN}/σ_R values, the other with $\sigma_{CN}/\sigma_R = 1$. Sikkeland obtained fits of statistical theory to experimental data by adjusting the fission barrier B_f and the ratio of the level density parameter for fission, a_f, to that for neutron emission, a_n. Our procedure is analogous in that respect, since we also adjust the magnitude of the fission barrier and of a_f/a_ν, where a_ν is the level density parameter for particle emission in general. In our procedure, however, while the absolute value of the fission barrier is a free parameter, its angular-momentum dependence is given by the liquid-drop model. As was mentioned in section III, σ_R is obtained using parabolic potentials due to Thomas [20]. This latter procedure can be justified on the basis of experimental results of Viola and Sikkeland [7].

In fig. 10 we show our calculated fits to the data of ref. 5, in which we have assumed the same σ_{CN}/σ_R values as Sikkeland. The theoretical fits to experimental data appear to be somewhat better than those shown in fig. 9. More important than the quality of the fits, however, are the parameters associated with them. These are given in table I both for our fits and for those of ref. 5.

TABLE I

Excitation function parameters for fission of compound nucleus ^{181}Re

	This work $\sigma_{CN} = \sigma_R$		This work $\sigma_{CN} = f\sigma_R$		Sikkeland [5] $\sigma_{CN} = f\sigma_R$	
	B_f (MeV)	a_f/a_ν	B_f (MeV)	a_f/a_ν	B_f (MeV)	a_f/a_ν
$^{169}Tm+^{12}C$	20.1	1.01	21.0	1.08	24.0	1.20
$^{165}Ho+^{16}O$	18.8	1.005	19.7	1.08	23.9	1.21
$^{159}Tb+^{22}Ne$	16.8	0.98	19.7	1.12	24.3	1.25

σ_{CN} is the estimated compound nucleus cross section, σ_R is the calculated total reaction cross section, B_f is the fission barrier for zero angular momentum, a_f/a_ν is the ratio of level density parameter for fission to that for particle emission, and f has the values 0.72 for the ^{12}C and ^{16}O reactions, and 0.6 for the ^{22}Ne case.

If we compare results for $\sigma_{CN} = f\sigma_R$, it can be seen that our extracted fission barrier is on the average 8% lower than that of Sikkeland. If we change our assumption regarding the compound nucleus cross section and consider the case $\sigma_{CN} = \sigma_R$, the uncertainty in the extracted fission barrier increases still further. Since the same compound nucleus is presumably formed in the three reactions given in the table, the fission barriers extracted from the three excitation functions should be identical. It can be seen that this is not the case

for any of the fits considered in table I. We have to conclude that, in the absence of a precise knowledge of σ_{CN}, the situation with regard to the deduction of fission barriers from heavy-ion excitation functions is rather unsatisfactory. This comment applies to all barriers obtained in refs. 5 and 6. I feel that our fission barriers for any particular value of σ_{CN}/σ_R are more realistic than Sikkeland's, but due to the sensitivity of the whole procedure to the value of σ_{CN}/σ_R, reliable barriers will probably not be available until σ_{CN} results are obtained by including measurements of evaporation residue cross sections.

Recently we have obtained data on the fission of ^{153}Tb produced in ^{12}C bombardments of ^{141}Pr and ^{20}Ne bombardments of ^{133}Cs [32]. The results are shown in fig. 11, together with theoretical fits to the data, on the assumption that $\sigma_{CN} = \sigma_R$. The solid lines are "best" fits in which the non-rotating fission barrier was found to be equal to 27.4 MeV for both reactions, and in which values of a_f/a_ν were 0.97 for the ^{12}C case and 1.00 for the ^{20}Ne case. Since there is no theoretical reason why a_f/a_ν values should be different in the two cases, we have also indicated by means of dashed lines "compromise" fits to both sets of data, in which B_f = 27.4 MeV and a_f/a_ν = 0.98. We can conclude that, with the assumption $\sigma_{CN} = \sigma_R$, the angular-momentum-dependent lowering of B_f (used in our analysis) can account for a fair fraction of the observed difference in fissility between the ^{20}Ne + ^{133}Cs system and the ^{12}C + ^{141}Pr system, but not for all of the observed difference.

The above conclusion may again, however, be strongly influenced by assumptions regarding σ_{CN}/σ_R. This point can be made with reference to fig. 12 which, in the lower half, shows partial reaction cross sections for the two systems. The total excitation energy is about 85.5 MeV in both cases, and the fission barrier is shown for reference. In the upper part of fig. 12, the calculated fission cross sections are shown as a function of angular momentum for B_f = 27.4 and a_f/a_ν = 0.98 (corresponding to the dashed curves of fig. 11). The salient feature is that while the spin distribution in the ^{20}Ne case extends only about 5$\hbar$ beyond that of the ^{12}C case, and while the fission barrier in that angular momentum region is decreasing only at the rate of about 2 MeV per 5$\hbar$, the effect on the fission cross section is rather large, as can be seen in the top part of the figure.

Furthermore, most of the fission is expected to be associated with a rather narrow band of the highest partial waves. The importance of what one assumes about these highest partial waves is thus evident. We must remember that processes that do not lead to compound nucleus formation are also likely to involve the highest partial waves. Thus we may expect the fission excitation function to be sensitive not only to the ratio σ_{CN}/σ_R, but also to the functional forms of the angular momentum cutoff on $\sigma_{CN}(J)$, where $\sigma_{CN}(J)$ is the partial compound nucleus formation cross section. For most purposes it has been customary to use the sharp-cutoff approximation, in which the total compound nucleus cross section σ_{CN} is given by

$$\sigma_{CN} = \sum_{J=0}^{J_{crit}} \sigma_R(J)$$

where $\sigma_R(J)$ is the partial reaction cross section, and J_{crit} is a critical value of angular momentum. As will be indicated below, it is possible that in the case of the ^{127}La compound nucleus the $\sigma_{CN}(J)$ cutoff is, in fact, not sharp.

The final case that I would like to discuss in this section is the fission of ^{107}Ag induced with ^{20}Ne ions [31]. The data points are shown in fig. 13, connected by a heavy solid line to guide the eye. In our original analysis of the data, based on the assumption that $\sigma_{CN} = \sigma_R$, we did not find it possible to obtain a fit by the method discussed above. The series of thin lines in fig. 13 illustrates this point. They represent fits to the lowest data point and involve barriers ranging from 110% (curve A) to 60% (curve F) of the liquid-drop values.

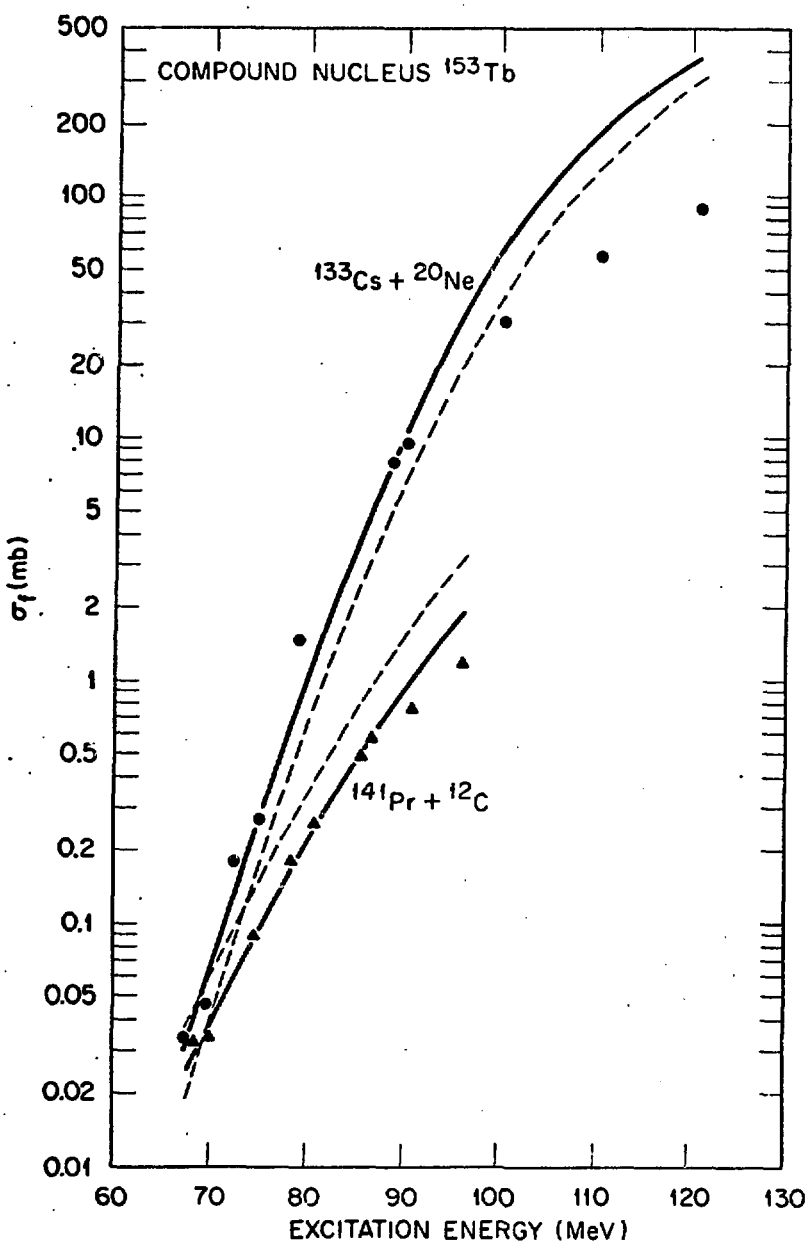

Figure 11. Experimental and calculated fission excitation functions for the fission of the ^{153}Tb compound nucleus produced in two different ways [32]. The solid curves represent best fits to data. The dashed curves represent a simultaneous fit to both sets of data in which the parameters are required to be the same for the two reactions (see text).

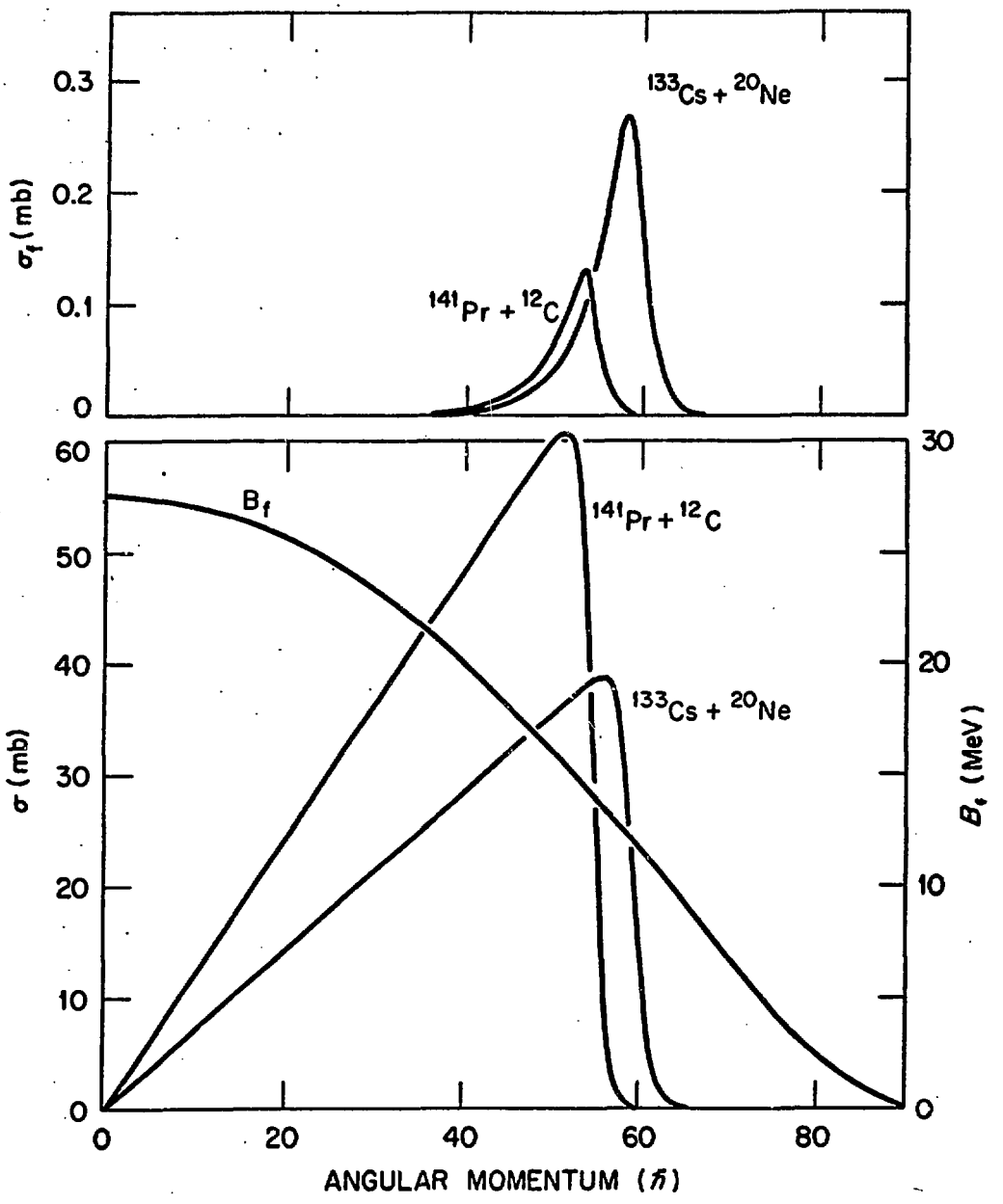

Figure 12. In the lower section, partial reaction cross sections are shown for two reactions both producing the ^{153}Tb compound nucleus at an excitation energy of about 85.5 MeV. In the upper portion, the corresponding calculated partial fission cross sections are shown. The fission barrier for ^{153}Tb is given in the lower part of the figure for reference. (See text for details.)

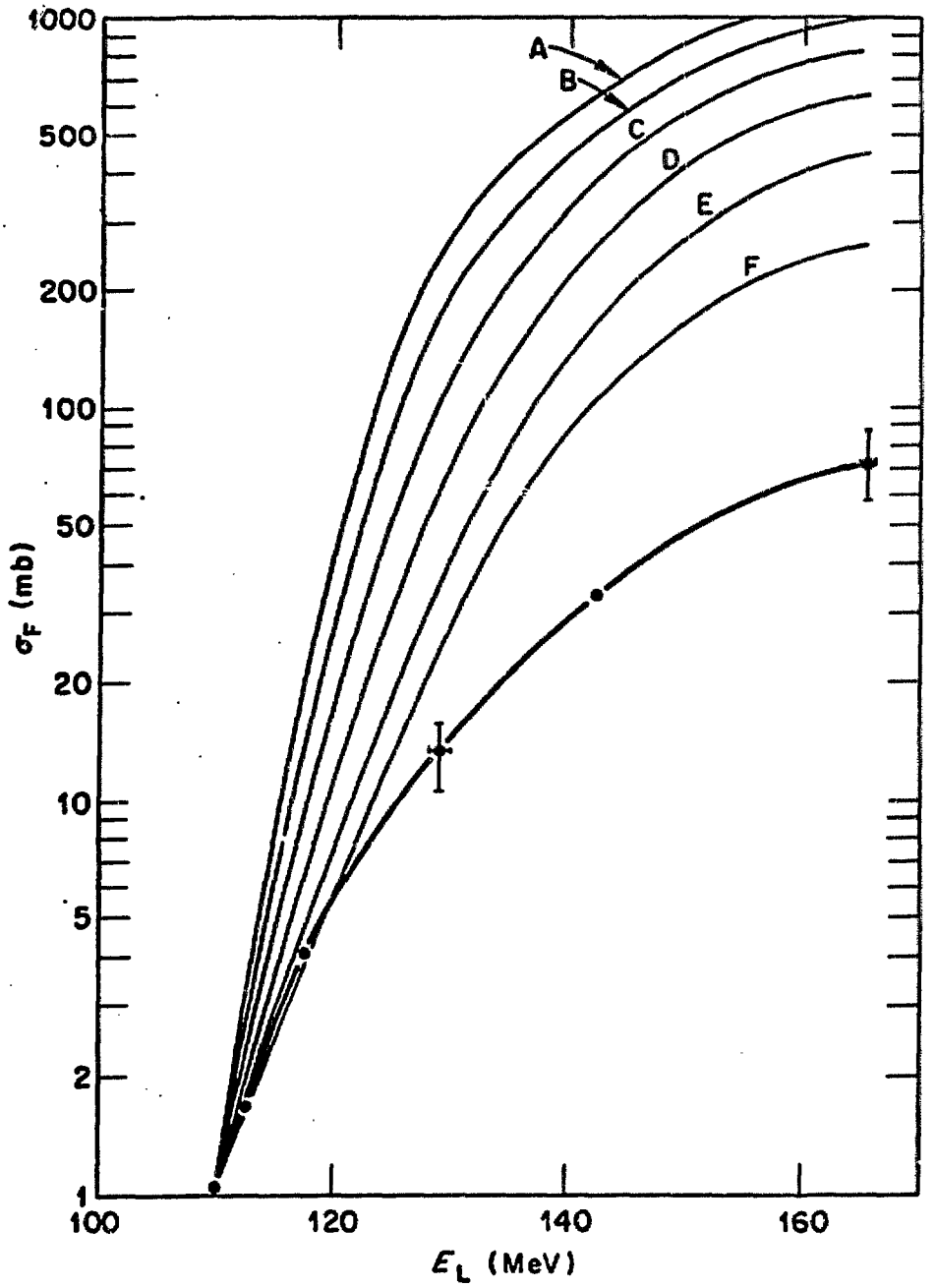

Figure 13. Measured fission excitation function (closed circles and heavy solid line), and attempted theoretical fits for the reaction $^{107}Ag + {}^{20}Ne \rightarrow {}^{127}La \rightarrow$ fission. The fission barrier was varied from 110% of the liquid drop value in curve A to 60% of the liquid drop value in curve F. This figure is taken from ref. 3.

As I have shown above, the data analysis is rather sensitive to the ratio σ_{CN}/σ_R, and we have, therefore, recently measured the evaporation residue cross sections σ_{ER} [33]. In this region of relatively light nuclei it is safe to assume that $\sigma_{CN} = \sigma_{ER} + \sigma_F$, where σ_F is the fission cross section; our experimental σ_{CN} results are shown in the upper section of fig. 14. Cases such as this, where σ_F and σ_{CN} are both determined experimentally, should, in principle, be the most favorable ones for our method of data analysis. Zebelman et al. [35] also have measured both σ_F and σ_{CN} for several cases, and have found their data consistent with a theoretical treatment similar to ours. Their measurements, however were performed at only one bombarding energy in each case; their analysis, therefore, was not subjected to the additional constraint of describing an entire excitation function.

The results of our analysis of the ^{127}La fission excitation function resulting from the bombardment of ^{107}Ag with ^{20}Ne are given in the lower part of fig. 14. The experimental points are again shown with a heavy solid line connecting them. Fits were forced to pass through the data point at 128.5 MeV bombarding energy. The fission barrier ranges from 60% of the liquid drop value (curve A) to 100% of the liquid drop value (curve E). Once again, a satisfactory fit was not obtained. We have considered the possibility that certain very asymmetric fission events did not register in our coincident-fragment detector system and that our experimental results are, therefore, in error. This possibility was rejected, however, on the basis of ΔE - E telescope results in which coincidence between fragment pairs was not required, and in which a clean separation was obtained between fission and transfer products.

It is difficult to think of physical effects that can reproduce the rather shallow slope of the measured fission excitation function. One way, however, in which it may be possible to explain the results is by replacing the sharp-cutoff approximation, which was used in the data analysis, by a sloping-cutoff. As was discussed earlier, in the sharp cutoff approximation, $\sigma_{CN}(J) = \sigma_R(J)$ up to some value of J_{crit} above which $\sigma_{CN}(J) = 0$. It is possible to modify this approximation in such a way that $\sigma_{CN}(J) = \sigma_R(J)$ only up to some point below J_{crit}. Above this point $\sigma_{CN}(J)$ would decrease linearly as a function of J up to some other point located above J_{crit}. With such an assumption the experimental results may perhaps be understood, and we intend to investigate this possibility in the future.

To summarize this section, the extraction of fission barriers from heavy-ion-induced fission data is complicated by the fact that, in most cases, measurements of evaporation-residue products are not available. The published fission barriers obtained from heavy-ion-induced fission are probably unreliable, and should be regarded with caution. The increasing fissility with increasing angular momentum can be understood qualitatively in terms of a decreasing fission barrier, but there are some quantitative problems. These may be related to the prediction that fission is very sensitive to the highest possible partial waves. For the lightest system studied, in which both the fission and the compound nucleus formation excitation functions have been measured, there are serious discrepancies between our data and the theoretical treatment. This may indicate that the sharp-cutoff approximation is not valid.

V. Fragment Mass and Total Kinetic Energy Distributions

The earliest fragment kinetic energy measurements are due to Viola and Sikkeland [4] who measured single fragment energies from ^{12}C and ^{16}O-induced fission of targets ranging from ^{141}Pr to ^{240}Pu. Somewhat later, Plasil et al. [36] measured kinetic energies of coincident fragment pairs and extracted mass and total kinetic energy distributions for ^{4}He, ^{12}C and ^{16}O-induced fission of ^{170}Er, ^{174}Yb, and ^{182}W. Typical fragment distributions from ref. 36 are shown in fig. 15. The data are from the fission of the compound nucleus ^{186}Os produced in ^{4}He-bombardments of ^{182}W and in ^{16}O-bombardments of ^{170}Er. The laboratory

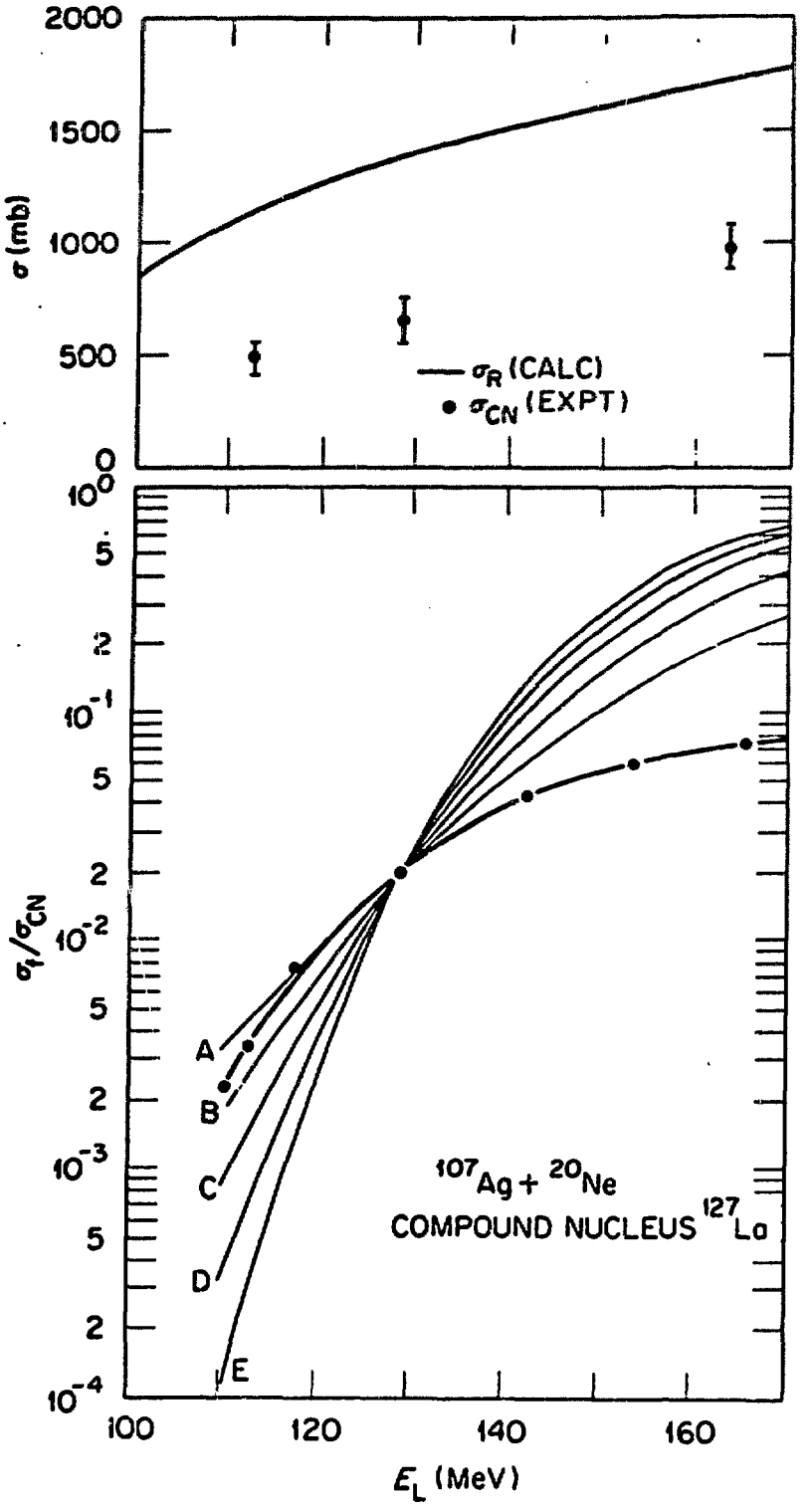

Figure 14. In the top part of the figure the calculated total reaction cross section is shown for $^{107}Ag + {}^{20}Ne \rightarrow {}^{127}La$ as a function of laboratory bombarding energy. Also shown are three data points for the measured compound nucleus cross section σ_{CN}, where $\sigma_{CN} = \sigma_{ER} + \sigma_F$ [33]. In the bottom part of the figure several attempted theoretical fits (thin lines) to fission excitation functions are shown. (See text for further details.)

bombarding energies E_L were chosen so as to give the same compound nucleus excitation energy. It can be seen that the mass distribution peaks at symmetric mass divisions, which is a feature that applies to most heavy-ion-induced fission cases, ranging from $^{107}Ag + ^{20}Ne$ [31] to $^{246}Cm + ^{18}O$ [37]. The qualitative effect of angular momentum, shown in fig. 15, is that as angular momentum increases, the widths of both the mass and the total kinetic energy distributions increase. Also shown in fig. 15 are theoretical calculations of Nix and Swiatecki [38], which are based on the dynamic liquid-drop model. Theoretical and experimental results are in good agreement.

An example of a contour diagram of fragment mass vs. fragment total kinetic energy is shown in fig. 16 for one of the lightest systems studied [31]. The triangular appearance of such contour plots is characteristic for all heavy-ion-induced fission cases that involve full momentum transfer from projectile to the fissioning system [31,36,39]. A qualitative explanation of the triangular shape is that for large total kinetic energies, the fissioning system is subject to more stringent constraints, resulting in a relatively narrow mass distribution.

Systematic trends of the statistical moments of the fragment distributions with increasing angular momentum are not very well established. Table II presents results for the ^{186}Os compound nucleus of Plasil et al. [36] and for the

TABLE II

Moments of mass and total kinetic energy distributions from the fission of ^{186}Os and ^{210}Po compound nuclei

System	E_L (MeV)	E_X (MeV)	$\langle E_K \rangle$ (MeV)	$\sigma^2_{E_K}$ (MeV^2)	σ^2_M (amu^2)	Reference
$^{182}W + ^{4}He = ^{186}Os^*$	100	95.0	125	67	200	36
$^{170}Er + ^{16}O = ^{186}Os^*$	127.8†	95.0	124	93†	205†	36
$^{206}Pb + ^{4}He = ^{210}Po^*$	63.8	57.2	147	69	132	40
$^{198}Pt + ^{12}C = ^{210}Po^*$	77.2	58.5	151.6	73	140	40

In this table E_L is the laboratory bombarding energy, E_X is the excitation energy, $\langle E_K \rangle$ is the average fission total kinetic energy, $\sigma^2_{E_K}$ is the variance of the total kinetic energy distribution, σ^2_M is the variance of the mass distribution, and † denotes interpolated results.

^{210}Po compound nucleus of Unik et al. [40]. It can be seen that Plasil et al. find essentially no angular momentum effect on the fragment average total kinetic energy, while Unik et al. find a difference of 4.6 MeV between their ^4He and ^{12}C results. The results for the width of the total kinetic energy distribution are in disagreement. Unik et al. find a change of only 4 MeV^2 in the variance of the total kinetic energy distribution, while Plasil et al. find a change of 26 MeV^2 for their system. The only agreement between the two sets of data is the width of the mass distribution. A small increase was obtained in both cases. It is possible that kinetic energy results of ref. 40 are more accurate than the earlier results of ref. 36. On the other hand, results of Ngô, Péter and Tamain presented at this conference [41] seem to support the conclusions of ref. 36 rather than those of ref. 40.

Recently, fragment total kinetic energies of very heavy fissioning systems have been studied [37,42]. The motivation for these studies was provided by predictions of Schmitt and Mosel [43]. Based on a static scission model, they predict anomalously high fragment kinetic energies for fissioning nuclei in the mass region between 260 and 270 amu. Their calculations are shown in fig. 17 together with the experimental results of Ferguson et al. [37]. The predicted effect was not observed in the ^{18}O-induced fission of ^{246}Cm. This negative result,

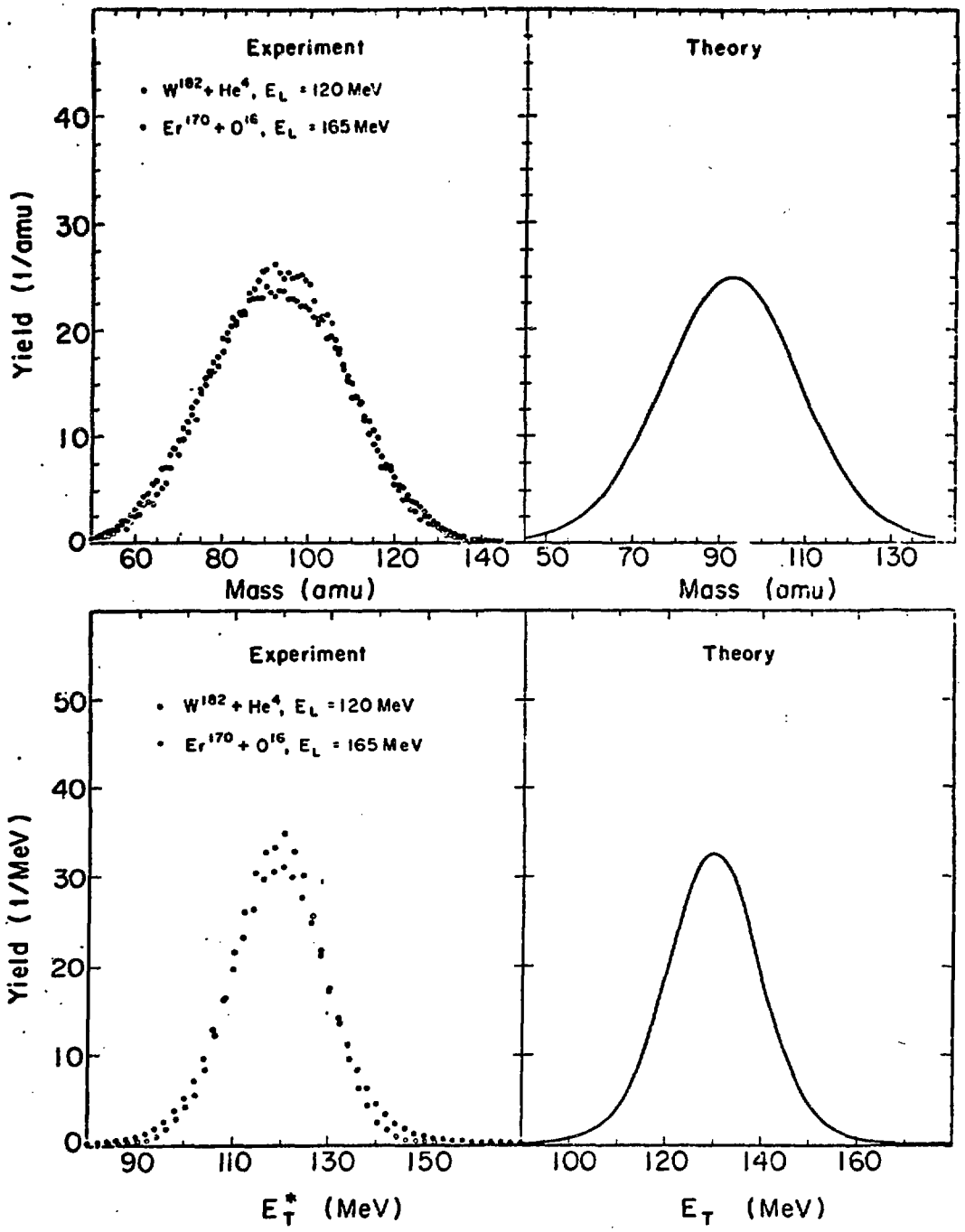

Figure 15. Experimental fragment yield-mass and yield-total kinetic energy curves from the fission of the ^{186}Os compound nucleus produced in ^{4}He and ^{16}O bombardments as indicated. Theoretical curves of Nix and Swiatecki [38] are also shown. The units of yield are arbitrary. This figure is taken from Plasil et al. [36].

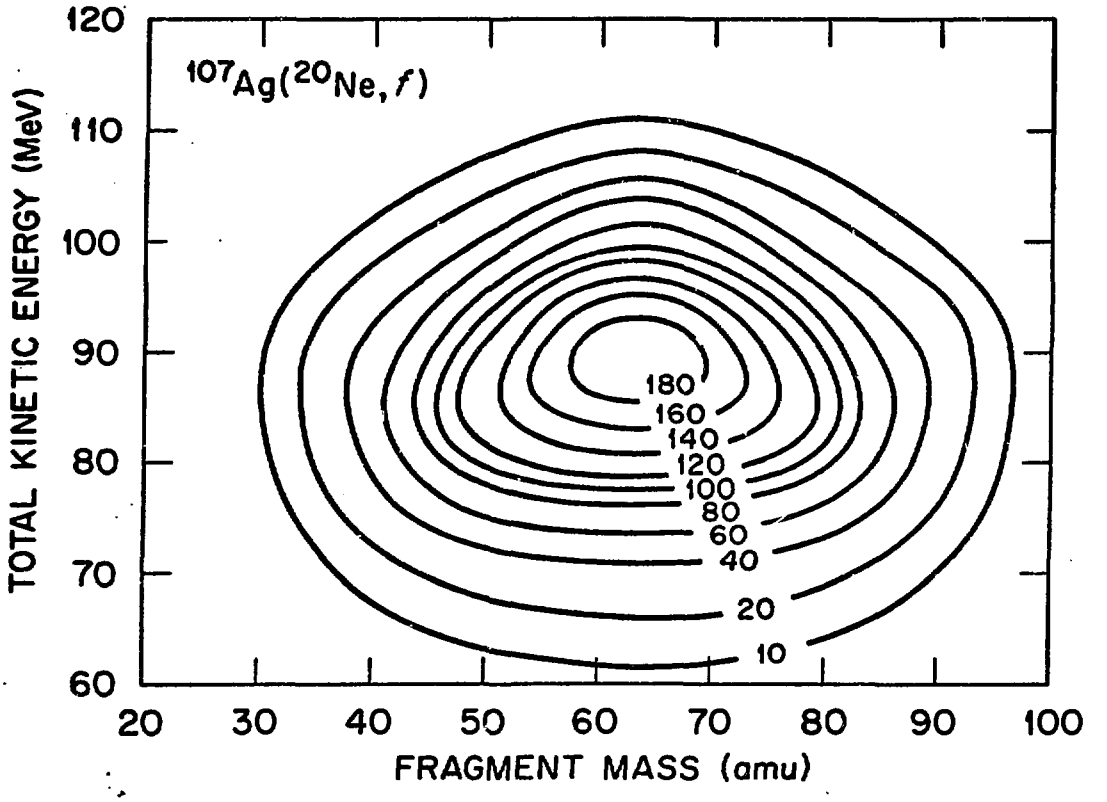

Figure 16. Fragment mass vs. total kinetic energy contour diagram. The labels on the contours refer to numbers of events in regions of 5 MeV by 5 amu. The data were symmetrized and smoothed. This figure is from ref. 31.

supported by results of ref. 42, is perhaps not surprising, since the predicted high kinetic energies are due to fragment shell effects, which are likely to be obscured by the high excitation energies involved in heavy-ion reactions. This is one of the reasons why we have not been concerned with such subjects as shell effects on the fission barrier in this review paper.

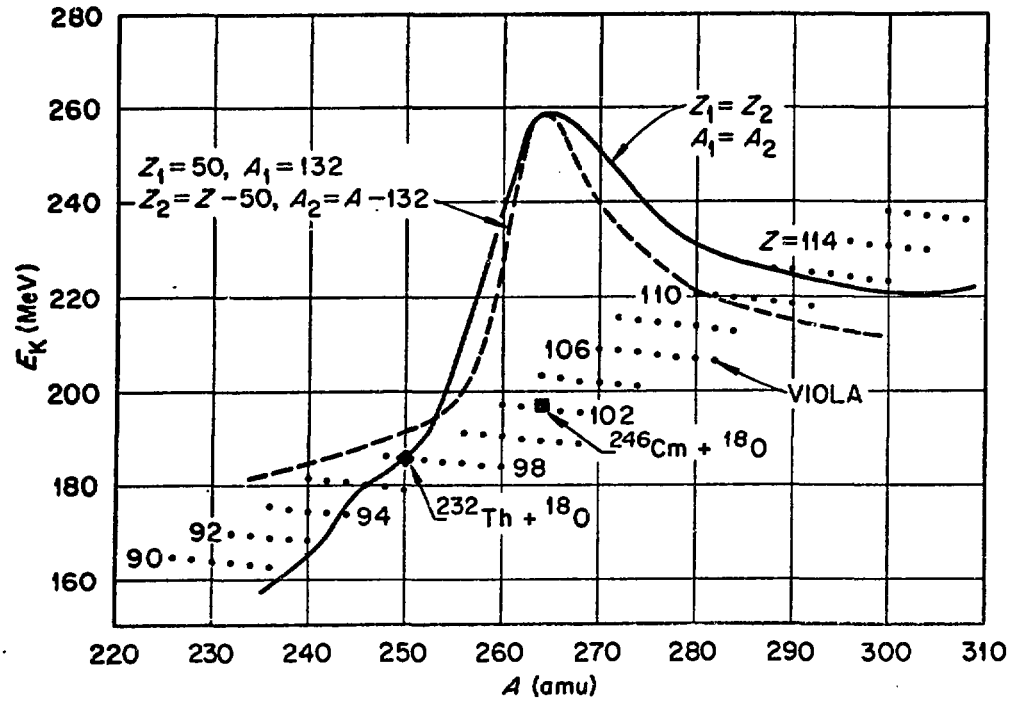

Figure 17. Comparison of predicted total fragment kinetic energy as a function of compound nucleus mass. The solid and dashed curves are the predictions of Schmitt and Mosel [43] for two different fragment mass divisions. The dots indicate the fission systematics of Viola [44]. The closed diamond and the closed square represent experimental pre-neutron emission results for the ^{232}Th and ^{246}Cm bombardments respectively [37]. This figure is taken from ref. 37.

VI. Non-Compound and "Quasi" Fission

In this section I shall discuss briefly those fission phenomena that do not involve the compound nucleus (see fig. 1). This is at the present time a very active field of research, and thus a comprehensive review is not possible. I will, therefore, discuss only a few selected examples. Early in the studies of heavy-ion-induced fission, Sikkeland, Haines and Viola [8] found interesting structure in their measured fission fragment angular correlations. They detected coincident fragment pairs with two well-collimated detectors from the heavy-ion-induced fission of targets ranging from ^{165}Ho to ^{238}U. If one detector is fixed and the angle of the other detector is varied, a peak is obtained at a kinematic angle that corresponds to full momentum transfer from the projectile to the target-plus-projectile system. For very fissile systems, however, Sikkeland et al. observed a shoulder or even a second peak in the angular correlation. An example of their results is given in fig. 18 for the case of ^{20}Ne-induced fission of ^{238}U. The second peak near 80° is consistent with momentum transferred by a ^{4}He ion. Thus it is likely that the observed fission fragments at that angle

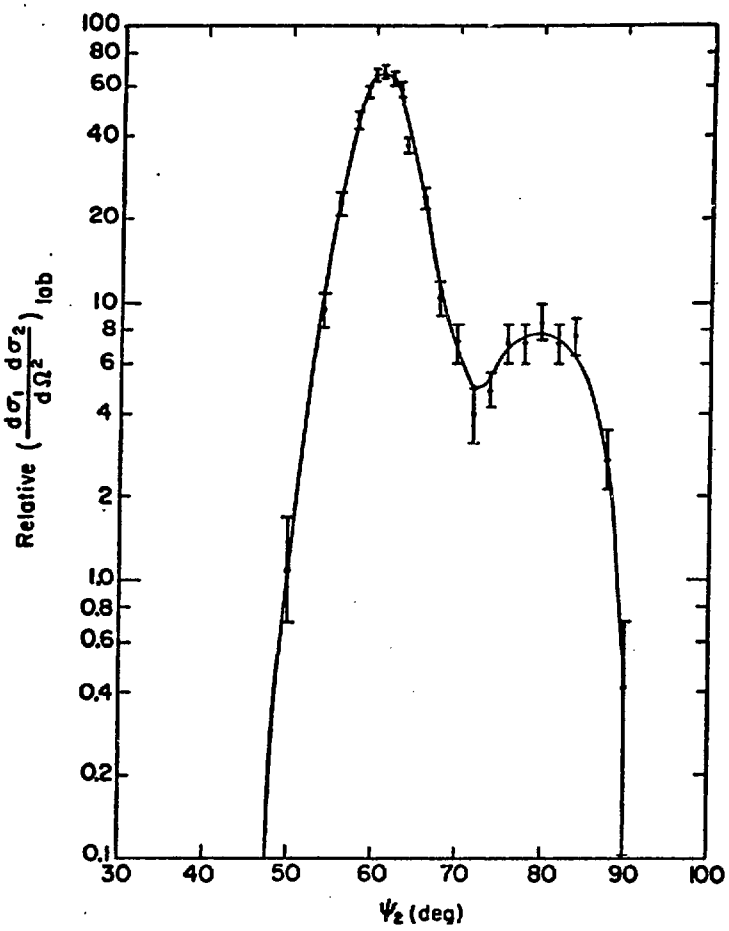

Figure 18. Fission fragment angular correlation for 207 MeV ^{20}Ne-induced fission of ^{238}U. One detector was fixed at 90° in the laboratory system, the other detector angle is given on the abscissa. This figure is taken from ref. 8.

are primarily due to fission following alpha transfer.

It was assumed by Sikkeland et al. [8] that the main peak in the angular correlation is due to the fission of the compound nucleus. As was discussed in section I, however, this is not necessarily true. What can be said for certain is that full momentum was transferred from the projectile to the composite system. It does not follow that all degrees of freedom were equilibrated before fission took place. It is possible that a more sensitive measure of whether or not a compound nucleus was formed is the shape of the fragment angular distribution. If the distribution has a $1/\sin\theta$ shape with no forward-peaking, it is an indication that the composite system has survived sufficiently long to undergo one or more rotations.

Very interesting results from argon and krypton-induced fission have been reported in the last year by Péter et al. [39]. Figure 19 illustrates their findings for $^{165}Ho + {}^{84}Kr$ and for $^{209}Bi + {}^{40}Ar$. In the lower part of the figure, the familiar triangular mass vs. total kinetic energy distribution is shown for the ^{40}Ar bombardment. In the upper part of the figure, which gives the results for the ^{84}Kr case, it can be seen that the triangular fission distribution has been replaced by a distribution of fragments that typically have masses similar to the masses of target and projectile nuclei. The energies of the fragments, however, are more nearly consistent with Coulomb repulsion between fission fragments than with transfer reactions. In another case discussed in ref. 39, it was found that 500-MeV ^{84}Kr bombardments of ^{209}Bi yielded essentially no fragments corresponding to symmetric fission, but a number of fragments with masses near those of the projectile and the target were observed. These fragments also had energies characteristic of Coulomb repulsion.

Recently, similar results were obtained by a group of outside-users at the Lawrence Berkeley Laboratory [45] with a 600-MeV ^{84}Kr beam incident on ^{209}Bi. Based on preliminary results, they found at this higher energy that the cross section for full-momentum-transfer fission was much higher than at lower Kr energies, but that it still accounted for a relatively minor fraction of the total reaction cross section. They also found that, at this bombarding energy, a major fraction of the total reaction cross section appeared as the deep inelastic process or quasi-fission discussed above, and that the angular distribution for this process had a well-defined peak centered near the grazing angle. Similar results on the angular distribution of quasi-fission fragments have been reported at this conference [46], and are discussed by W. D. Myers in this volume of the proceedings.

To end, I would like to report on some preliminary data obtained by us in an experiment at the Lawrence Berkeley Laboratory [47]. The data are shown in table III. The two systems studied are $^{40}Ar + {}^{109}Ag$ and $^{84}Kr + {}^{65}Cu$, both giving

TABLE III
Comparison of ^{40}Ar and ^{84}Kr bombardments leading to the same composite system

Reaction	Compound Nucleus	E_{lab} (MeV)	E_x (MeV)	σ_R (mb)	σ_{ER} (mb)	σ_F (mb)	ℓ_{crit}(ER) ($\hbar$)
$^{40}Ar+{}^{109}Ag$	^{149}Tb	288	158.3	1770	700*	600*	81
$^{84}Kr+{}^{65}Cu$	^{149}Tb	605	185.6	1860	400*	1300*	77

In this table E_{lab} is the laboratory bombarding energy, E_x is the compound nucleus excitation energy, σ_R is the calculated total reaction cross section, σ_{ER} is the measured cross section for evaporation residue products, σ_F is the measured fission cross section, and ℓ_{crit}(ER) is a critical angular momentum deduced from σ_{ER} via the sharp cutoff model. The asterisk indicates preliminary data.

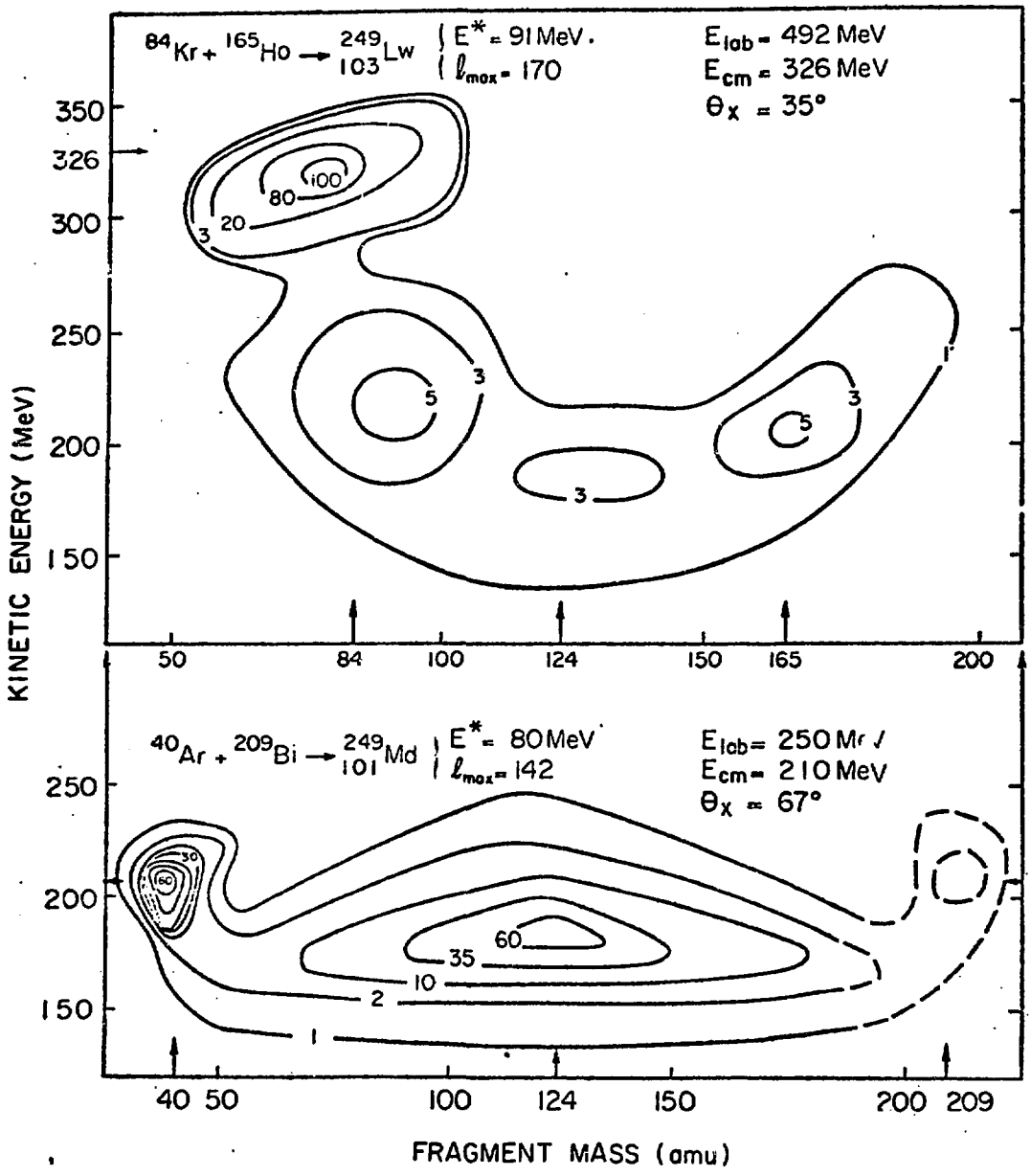

Figure 19. Fragment mass vs. total kinetic contour diagrams for ^{84}Kr + ^{165}Ho and ^{40}Ar + ^{209}Bi from ref. 39. E^* is the total excitation energy, E_{cm} is the center-of-mass bombarding energy, E_{lab} is the bombarding energy in the laboratory system, ℓ_{max} is the maximum angular momentum involved in the reaction and $\pm \theta_x$ are the angles with respect to the beam at which the two fission detectors are positioned.

the composite system ^{149}Tb. It can be seen that similar excitation energies and calculated total reaction cross sections are involved in the two cases. The most striking difference between the two reactions is that the fission cross section is much larger in the ^{84}Kr case than in the ^{40}Ar case. In the Ar bombardment, the sum of σ_{ER} and σ_F falls about 500 mb short of the calculated σ_R. As was mentioned earlier, the 500 mb can probably be accounted for by simple transfer processes [24]. In the Kr case, on the other hand, $\sigma_{ER} + \sigma_F$ falls only 160 mb short of σ_R. In view of the large σ_F in this case, it is possible that some of the fission events are due to "direct" or "fast" fission of the composite system, which may be analogous to the quasi-fission observed in bombardments of heavier targets.

VII. Summary

The field of heavy-ion-induced fission is dominated by the fact that fission barriers decrease as angular momentum increases. Estimates of the angular-momentum dependence of the barriers can be made in the framework of the rotating-liquid-drop model. Compound-nucleus de-excitation calculations that include angular-momentum-dependent fission barriers can be used to predict cross sections for evaporation-residue products and to analyze fission excitation functions. Previously published fission barriers may be in error, and σ_{ER} measurements are needed before better values for barriers can be obtained with existing fission data. The general features of fission excitation functions are understood, but there are quantitative problems that remain to be settled. The fission excitation function for ^{127}La presents a special problem and may indicate that the sharp-cutoff approximation is not valid. Data are available on fragment-mass and kinetic-energy distributions, but no coherent pattern emerges, except that shell effects are probably not important at the high excitation energies characteristic of heavy-ion reactions. An exciting field of research on non-compound-nucleus fission has opened up with the availability of very heavy projectiles such as Kr.

Acknowledgements

I would like to thank my colleagues, R. L. Ferguson, F. Pleasonton, R. L. Hahn, M. Blann, H. C. Britt, B. H. Erkkila, H. H. Gutbrod and R. H. Stokes for permission to use experimental results prior to publication. I am grateful to M. Blann, H. C. Britt, R. L. Ferguson, H. H. Gutbrod, J. Miller, W. D. Myers, J. R. Nix, W. J. Swiatecki, J. P. Unik and K. L. Wolf for helpful discussions. I would like to thank R. L. Ferguson for a critical reading of the manuscript.

References

[1] For a recent review of nuclear fission, see H. J. Specht in Proceedings of the International Conference on Nuclear Physics, Munich, August 1973.

[2] M. Blann and F. Plasil, Phys. Rev. Lett. 29 (1972) 303.

[3] F. Plasil and M. Blann, to be published.

[4] V. E. Viola, Jr. and T. Sikkeland, Phys. Rev. 130 (1963) 2044, and T. Sikkeland, Phys. Lett. 31B (1970) 451.

[5] T. Sikkeland, Phys. Rev. 135 (1964) B669.

[6] T. Sikkeland, J. E. Clarkson, N. H. Steiger-Shafrir, and V. E. Viola, Jr., Phys. Rev. C3 (1971) 329.

[7] V. E. Viola, Jr. and T. Sikkeland, Phys. Rev. 128 (1962) 767.

[8] T. Sikkeland, E. L. Haines and V. E. Viola, Jr., Phys. Rev. 125 (1962) 1350.

[9] T. Sikkeland, Phys. Lett. 27B (1968) 277.

[10] G. E. Gordon, A. E. Larsh, T. Sikkeland and G. T. Seaborg, Phys. Rev. 120 (1960) 1341.

[11] G. A. Pik-Pichak, J. Exptl. Theoret. Phys. (U.S.S.R.) 34 (1958) 341, translated in Soviet Phys. JETP 34 (1958) 238; J. Exptl. Theor. Phys. (U.S.S.R.) 42 (1962) 1294, translated in Soviet Phys. JETP 15 (1962) 897; J. Exptl. Theor. Phys. (U.S.S.R.) 43 (1962) 1701, translated in Soviet Phys. JETP 16 (1963) 1201.

[12] R. Beringer and W. J. Knox, Phys. Rev. 121 (1961) 1195.

[13] J. R. Hiskes, "The Liquid Drop Model of Fission Equilibrium Configurations and Energetics of Uniformly Rotating Charged Drops," University of California Lawrence Radiation Laboratory Report UCRL-9275 (1960).

[14] S. Cohen, F. Plasil, and W. J. Swiatecki, "Proceedings Third Conference on Reactions Between Complex Nuclei" (A. Ghiorso, R. M. Diamond and H. E. Conzett, Eds.), p. 325, University of California Press, 1963; University of California Radiation Laboratory preprint UCRL-10775, 1963.

[15] S. Cohen, F. Plasil and W. J. Swiatecki, Ann. Phys. 82 (1974) 557.

[16] In a recent paper (paper DB3 given at the Spring Meeting of the American Physical Society in Washington, D.C., April 1974), L. G. Moretto has pointed out that for very large angular momenta and excitation energies such as are involved, for example, in 288 MeV ^{40}Ar bombardments of ^{109}Ag, the estimated neutron emission time is comparable to nuclear vibration and rotation times. Thus the whole compound nucleus concept must be viewed with caution in such cases.

[17] W. J. Swiatecki, private communication.

[18] R. F. Reising, G. L. Bate and J. R. Huizenga, Phys. Rev. 141 (1966) 1161.

[19] M. Blann and F. Plasil, "ALICE: A Nuclear Evaporation Code," U.S.A.E.C. report COO-3494-10, Nov. 1, 1973, (unpublished).

[20] T. D. Thomas, Phys. Rev. 116 (1959) 703.

[21] V. Weisskopf and D. H. Ewing, Phys. Rev. 57 (1940) 472.

[22] N. Bohr and J. A. Wheeler, Phys. Rev. 56 (1939) 426.

[23] H. H. Gutbrod, F. Plasil, H. C. Britt, B. H. Erkkila, R. H. Stokes and M. Blann, paper IAEA-SM-174/59 in Proc. Third IAEA Symposium on the Physics and Chemistry of Fission (Rochester, New York, August 1973).

[24] M. E. Hille, P. Hille, H. H. Gutbrod and M. Blann, private communication.

[25] M. Lefort, Y. LeBeyec and J. Péter, Riv. Nuovo Cimento 4 (1974) 1.

[26] H. Gauvin, Y. LeBeyec and N. T. Porile, Nucl. Phys. A223 (1974) 103.

[27] S. M. Polikanov and V. A. Druin, Zh. Eksperim. i Teor. Fiz. 36 (1959) 744 [English translation: Soviet Phys. JETP 9 (1959) 522].

[28] H. C. Britt and A. R. Quinton, in Proceedings of the Second Conference on Reactions Between Complex Nuclei, Gatlinburg, May 1960 (John Wiley & Sons, Inc., New York, 1960).

[29] E. Goldberg, H. L. Reynolds, and D. D. Kerlee, in Proceedings of the Second Conference on Reactions Between Complex Nuclei, Gatlinburg, May 1960 (John Wiley & Sons, Inc., New York, 1960).

[30] J. Gilmore, S. G. Thompson and I. Perlman, Phys. Rev. 128 (1962) 2276.

[31] F. Plasil, R. L. Ferguson and F. Pleasonton, paper IAEA-SM-174/71 in Proc. Third IAEA Symposium on the Physics and Chemistry of Fission (Rochester, New York, August 1973).

[32] F. Plasil, R. L. Ferguson and F. Pleasonton, to be published.

[33] F. Plasil, R. L. Ferguson, F. Pleasonton and R. L. Hahn, preliminary results.

[34] U. L. Businaro and S. Gallone, Nuovo Cimento 5 (1957) 315.

[35] A. M. Zebelman, K. Beg, Y. Eyal, G. Jaffe, D. Logan, J. Miller, A. Kandil and L. Kowalski, paper IAEA-SM-174/67 in Proc. Third IAEA Symposium on the Physics and Chemistry of Fission (Rochester, New York, August 1973); and R. L. Kozub, D. Logan, J. M. Miller and A. M. Zebelman, preprint April 1974.

[36] F. Plasil, D. S. Burnett, H. C. Britt and S. G. Thompson, Phys. Rev. 142 (1966) 696.

[37] R. L. Ferguson, F. Plasil, H. Freiesleben, C. E. Bemis, Jr., and H. W. Schmitt, Phys. Rev. C8 (1973) 1104.

[38] J. R. Nix and W. J. Swiatecki, Nucl. Phys. 71 (1965) 1.

[39] J. Péter, F. Hanappe, C. Ngô and B. Tamain, in Proceedings of the International Conference on Nuclear Physics, Munich, August 1973.

[40] J. P. Unik, J. G. Cuninghame, and I. F. Croall, in Proceedings of the Second International Symposium on the Physics and Chemistry of Fission (International Atomic Energy Agency, Vienna, 1969), p. 717.

[41] C. Ngô, J. Péter and B. Tamain, in Proceedings of the Conference on Reactions Between Complex Nuclei, Nashville, June 1974 (North-Holland, Amsterdam, 1974), p. 114.

[42] B. Borderie, F. Hanappe, C. Ngô, J. Péter and B. Tamain, Nucl. Phys. A220 (1974) 93.

[43] H. W. Schmitt and U. Mosel, Nucl. Phys. A186 (1972) 1.

[44] V. E. Viola, Jr., Nucl. Data A1 (1966) 391.

[45] H. Freiesleben, J. R. Huizenga, J. P. Unik, V. Viola, and K. L. Wolf, private communication.

[46] F. Hanappe, C. Ngô, J. Péter and B. Tamain, in Proceedings of the Conference on Reactions Between Complex Nuclei, Nashville, June 1974 (North-Holland, Amsterdam, 1974) p. 116.

[47] M. Blann, H. C. Britt, B. H. Erkkila, H. H. Gutbrod, F. Plasil and R. H. Stokes, preliminary results.